

Fabrics-Based Embroidered Passive Displacement Sensors for On-Body Applications

¹Yulong Liu, ²Miao Wang, ³Bingyi Xia, ^{4*}Terry Tao Ye
^{1,2,3,4}Southern University of Science and Technology, Shenzhen, China
*Corresponding author's email: yet@sustech.edu.cn

Abstract

Wearable electronic applications require flexible and aesthetic devices that can be naturally concealed with daily clothes. Embroidered sensors will be the perfect solution for these requirements because the devices can be seamlessly integrated with normal fabrics with soft and breathable structures. In this paper, we proposed a displacement sensor that can be directly embroidered with conductive yarns on fabrics using standard embroidery processes. The proposed sensor uses two mutually coupled embroidered coils (called coupling planar coils or CPC); displacement between the two coils will alter the mutual inductance. The sensor can be served as an NFC/RFID antenna to achieve battery-less sensing, i.e., connected with a passive transponder chip, the variation of inductance will modulate the amplitude and phase changes in coupled signals and can be further demodulated by the reading devices. Furthermore, this sensing mechanism is directional, restorable and can sense the directions in which the displacement occurs. Experiments demonstrate that this embroidered sensor exhibits a good, repeatable correlation between the displacement and its inductance. It can find its use in movement detection, medical monitoring, and many other wearable applications.

1 Introduction

Among different approaches of implementations of flexible electronics, embroidered devices provide an ideal solution for wearable applications because the devices can be seamlessly integrated with the fabrics with soft, breathable and flexible structures. The devices are expected to be fabricated in the standard embroidery processes and provide a natural and aesthetic experience for users [13].

Many embroidered electronic devices had already been successfully demonstrated. Using conductive yarns, resistors, inductors and interconnects have been implemented.

Many RF devices such as antennas can also be embroidered directly on clothes with conductive yarns [14, 5]. The performance of these embroidered devices varies with different embroidery technique (stitch direction, stitch density, and sewing pattern) as well as the electrical properties of the conductive yarns [10, 11, 3].

In this paper, we introduce a low-cost, embroidered, coupling planar coils (CPC) based displacement sensor that can be used to detect movement and stretching activities (such as monitoring breathing activity by placing on the chest). The sensor structure consists of two series-connected coils that are embroidered on two layers of fabrics on top of each other (Figure 2). The sensor can be fabricated using standard embroidery processes with off-the-shelf conductive yarns. The sensor not only can detect lateral displacement, but it can also distinguish the direction of the displacement as well.

The sensing mechanism is based on properties of the mutual inductance of two planar coils. When connected in series and the coupling magnetic fluxes of each coil are in the same orientation, the changes in the mutual inductance will double the changes of the equivalent inductance of the CPC. Therefore, the CPC structure will serve as an ideal displacement sensor for the movement between the two fabrics layers. Furthermore, the CPC inductor can work as an NFC antenna, connected with an NFC chip, the variations in the inductance will be modulated as frequency and phase changes of the signal, and achieve passive sensing through NFC (ISO14443, ISO15693) readers [7, 5].

Several inductive-based displacement sensors had been proposed and widely used in industrial sensing and automation. However, most of the inductive sensors are PCB-based and lack of flexibility, and their applications are limited. For example, a mutual inductive-based sensor is reported in [4], it uses two separated planar spiral coils printed on PCB and stacked on top of each other, one of two coils is stationary, the other is movable. When a displacement occurs between the two coils, the input inductance of the sensor is changed correspondingly. Researchers in [2] proposed an enhanced inductive displacement sensor by applying an additional stationary coil, which increases the sensing range and sensing linearity. In addition, the RFID/NFC based sensing system had been developed for monitoring or tracking health state in recent years [1, 6], however, the sensors implemented in such system are mostly resistor-typed, which lead to power consumption inefficiently.

In comparison, the embroidered CPC sensor proposed in this paper has the following advantages:

1. The two coils are connected in series and coupled to each other magnetically. The variation of the mutual inductance can actually double the variation of the equivalent inductance. This structure enhances the CPC's sensitivity significantly. The experimental results show that the sensitivity of inductance is better than any other inductive-based sensors with comparable size. (Inductance varies from 3.47 μH to 4.63 μH within 30 mm displacement.)
2. When connected to NFC/RFID chips as antennas, the CPC coils can be used as sensors through antenna impedance modulation. The sensors can work perpetually without the need of replacing batteries.
3. The fabrication of CPC sensors uses standard embroidery process, which has low manufacturing cost and can be aesthetically integrated to apparels.

The paper is organized as follows: Section 2 describes the basic mechanism of CPC inductor and its use in displacement sensing. The sensor is designed, simulated and prototyped in Section 3. Experiments and results are discussed in Section 4, followed by the future work perspectives in Section 5.

2 CPC Sensing Mechanism

2.1 Mutual Inductance of Coupling Inductors

When two inductors are coupling to each other, the magnetic flux generated by one inductor will induce current in the other inductor, this effect is known as mutual inductance.

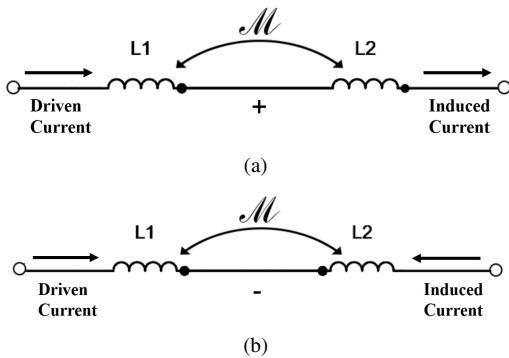


Figure 1. Mutual inductance and its polarity.

Connecting two coupled inductors in series, if the induced current is in the same direction as the driving current, as illustrated in Figure 1(a), the total equivalent inductance of these two inductors is:

$$L = L_1 + L_2 + 2M \quad (1)$$

Where L_1 and L_2 are the inductance of the two inductors respectively, and M is mutual inductance between these two inductors.

Similarly, if the induced current is in the opposite direction as the driving current flow, as illustrated in Figure 1(b), then the total equivalent inductance becomes:

$$L = L_1 + L_2 - 2M \quad (2)$$

The mutual inductance, M can be defined by the following equation:

$$M \propto \frac{d\Phi}{dt} \quad (3)$$

Where Φ is the magnetic flux between two coupling inductors. The value Φ is determined by many factors, including the geometry of each inductor, as well as the relative position and overlapping area of the coupled magnetic field. In fact, the sensing characteristics, such as linearity, are influenced by the geometry of coils as well, as illustrated by [9].

In summary, Eq.(1) and Eq.(2) demonstrates that the changes of the mutual inductance double the changes of the equivalent inductance of the two coupled inductors. Any factors that causes the variations of the mutual inductance can actually be magnified.

2.2 Stacked CPC Inductor

Connecting two coil-shaped planar inductors in series and stacking them on top of each other, the total equivalent inductance can either be increased or decreased by their mutual inductance, depending on the orientation of the coil and which terminals are connected. In our design, one coil's inner terminal is connected with the other coil's outer terminal, as illustrated in Figure 2(a), then the two coils are stacked on top of each other to form a pair of coupling inductors, as shown in Figure 2(b). The stacked coil-pair will form an equivalent inductor, with enhanced inductance from two remaining terminals.

When lateral displacement occurs between the two vertically stacked coils, as shown in Figure 2(c), their mutual inductance will be changed and consequently alter the total equivalent inductance, with the magnifying effect as discussed earlier. If the two coils are located at different layers that can move laterally, this coupling planar coil can be utilized to construct a lateral displacement sensor.

3 Design and Prototyping

3.1 Inductance of Planar Coils

The inductance of an inductor is mainly determined by its geometrical parameters. Wheeler's equation is widely used in the inductance estimation of these coil-shaped inductors [12]. In Wheeler's equation, different geometries, such as circular or square coil, have different coefficient factors. The estimation equations of circular-shaped coil and square-shaped coil are shown in Eq.(4) and Eq.(5) respectively. The geometrical parameters are illustrated in Figure 3.

$$L_{circle} = 31.33\mu_0 N^2 \frac{a^2}{8a + 11c} = 31.33\mu_0 N^2 \frac{a}{8 + 22\rho} \quad (4)$$

$$L_{square} = 2.34\mu_0 N^2 \frac{a^2}{a + 1.875c} = 2.34\mu_0 N^2 \frac{a}{1 + 2.75\rho} \quad (5)$$

Where μ_0 is the magnetic permeability of free space ($\mu_0 = 4\pi \times 10^{-7} \text{Hm}^{-1}$), N is the number of turns in the coil, a is

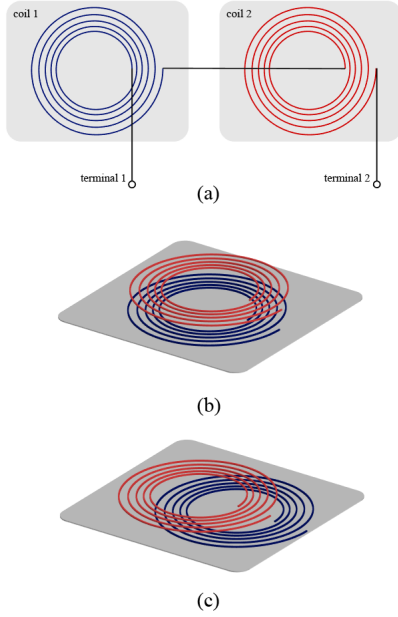


Figure 2. (a) Two coil-shaped planar inductors connected in series, (b) Stacked coupling coil structure and, (c) used as a displacement sensor.

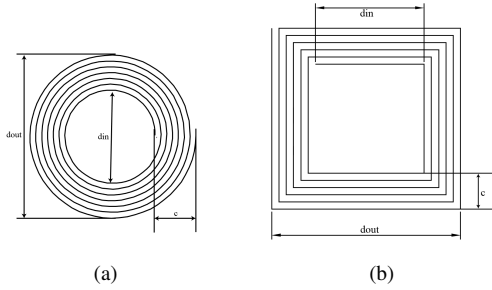


Figure 3. (a) Circular shaped, (b) square-shaped planar coil inductor and parameters for inductance estimation.

the average radius of the coil, where $a = \frac{d_{out} + d_{in}}{4}$, c is the distance between inner turn and outer turn, and ρ is defined as $\rho = \frac{d_{out} - d_{in}}{d_{out} + d_{in}}$.

We can use the above equations to estimate the inductance of planar coil inductors with different geometrical parameters.

3.2 Simulation of CPC Inductor

The mutual inductance between two coils of the stacked CPC inductor, as well as its total equivalent inductance, has been simulated. The impact of lateral displacement between the two planar coils has also been quantified in the simulation. Without loss of generality, circular planar coil designs are used in the simulation.

The geometrical parameters of each planar coil used in our simulation are shown in Figure 4. The CPC model consists of two circular coils of the same geometry, connected in series, as shown in Figure 1(a).

The geometrical parameters of the CPC model are listed

in Table 1, where r is the inner radius of the two coils, h is the vertical distance between them; d is the lateral displacement between the two coils along the y-axis. Both coils have the same number of turn n as well as track separation w . Additionally, a is the diameter of conducting thread used in the coil. The inner thread of the first coil is connected to the outer thread of the other one, thus the current will flow in the same direction for both coils and form an enhanced mutual inductance.

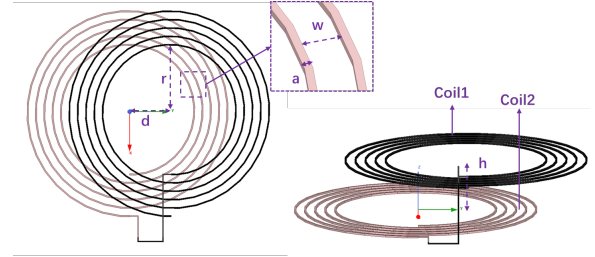


Figure 4. Design parameters and simulation setups of the CPC.

Table 1. Parameters of CPC inductors

| Parameters | r (mm) | h (mm) | n | w (mm) | a (mm) |
|------------|----------|----------|-----|----------|----------|
| Value | 15 | 3 | 5 | 2 | 0.48 |

The equivalent inductance of the CPC model under different displacement is simulated. From the results, we can see that the inductance is more sensitive under higher frequency, as shown in Figure 5. Specifically, the equivalent inductance L can be derived from the reactance in the measurements, by calculating $L = \frac{Im\{Z\}}{w}$. The inductance at 13.56 MHz is shown in Figure 6.

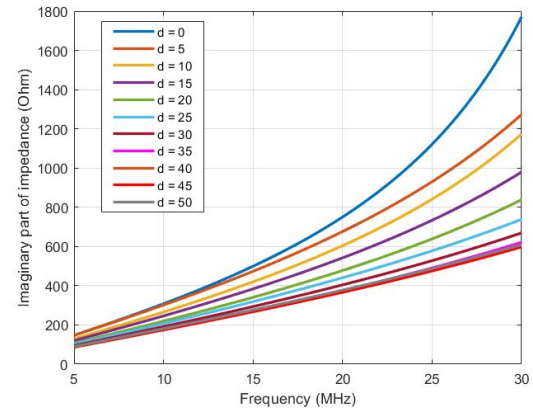


Figure 5. Impedance of CPC model under different displacement and frequencies.

To observe the magnetic field distribution of CPC inductors under different displacements, the magnetic field distribution maps are generated for three displacement scenarios, where $d = 0, 30,$ and 50 mm, respectively. The maps represent the field strength at 3 mm above the surface of Coil 1, as illustrated in Figure 7.

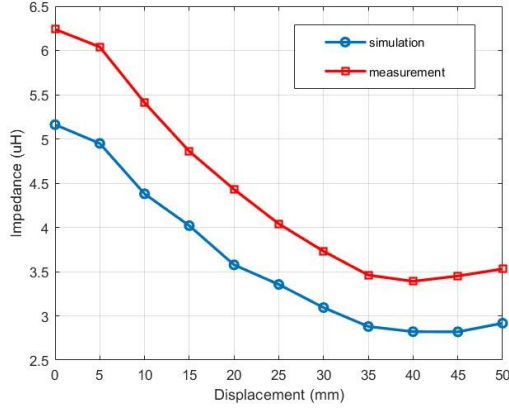


Figure 6. Simulation and measurement results of the equivalent inductance of CPC inductor with different displacements @13.56 MHz.

The illustrations demonstrated that the magnetic field is mostly concentrated inside the coil region, where the magnetic field is stronger in Coil 1 (shown in darker red), as compared to Coil 2 (shown in orange) due to the reference layer is near to Coil 1. The mutual inductance occurs in the overlapped region, as shown in Figure 7(b)(c), and the area of the overlapped region actually determines the intensity of the mutual inductance.

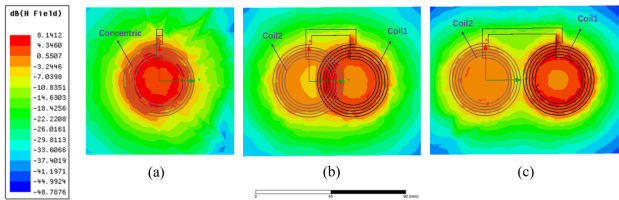


Figure 7. Magnetic field distribution between two coils of CPC with (a) $d=0$, (b) $d=30$, (c) $d=50$ (mm).

The simulation results show that the total equivalent inductance changes almost monotonically as the displacement increases, as shown in Figure 6. At the operating frequency of 13.56 MHz, the inductance varies from around 5.2 uH to 2.8 uH as the displacement changes from complete overlapping to complete detachment (0 mm to 50 mm). These results demonstrate that the proposed CPC inductor can be used as a reliable displacement sensor. In addition, an embroidered prototype with the same design parameters was fabricated and measured, the result can be seen in Figure 6 as well. The simulation and measurement results are off by a constant offset, but exhibit similar behavior under different displacements. The difference is attributed to the existence of parasitic capacitance in conductive yarns [8]. Although the simulation was conducted without considering the resistance of the threads, the results will still be valid when the coil are embroidered onto fabrics with conductive yarns.

3.3 Embroidered Planar Coils

In order to demonstrate the displacement sensing capabilities of CPC inductors, we have prototyped several embroi-

dered coils with circular and square shapes. Table 2 lists the geometrical parameters of these designs as well as the corresponding measured and calculated inductance, please note that the spacing distance between traces is set to be 2 mm in all designs.

Table 2. Design Parameters and Measured Inductance of Embroidered CPC @13.56MHz

| Geometry Type | d_{in} (mm) | d_{out} (mm) | Inductance Measured (μH) | Wheeler's Equation Calculated (μH) |
|---------------|---------------|----------------|---------------------------------------|-------------------------------------------------|
| Circular | 30 | 46 | 1.13 | 0.95 |
| Circular | 30 | 50 | 1.75 | 1.46 |
| Circular | 30 | 54 | 2.42 | 2.08 |
| Square | 30 | 46 | 1.30 | 0.57 |
| Square | 30 | 50 | 1.98 | 0.87 |
| Square | 30 | 54 | 2.70 | 1.24 |

In the embroidery process, the conductive yarns can be used as either the upper yarn or the lower yarn. In our case, the conductive yarns are served as lower bobbin to embroider continually on a non-conductive substrate.

The embroidery process is performed with a Brother commercial embroidery machine PR670E at the stitch rate of 400 rpm, and with a minimum stitch length of 1 mm. The non-conductive substrate is a woven cotton-flax fabric (thickness: 0.33 mm) and a layer of non-woven paper is placed underneath the woven fabric to support the embroidered geometry.

The conductive yarn used for the coil construction is a plied bundle of stainless-steel filaments. The yarn has a diameter of 0.48 mm, with resistivity of about 9.3 ohm/m.

Figure 8 shows the fabricated prototypes of square and circular planar coils in front and back side views as well as a finished CPC displacement sensor formed by two circular coils with 5 turns.

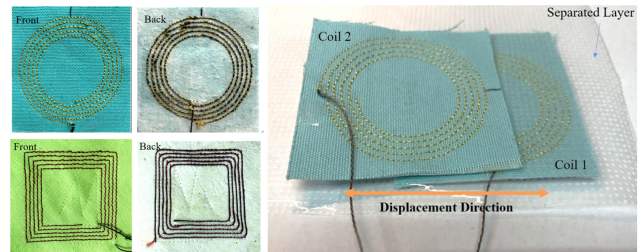


Figure 8. Embroidered CPC sensor prototypes.

4 Experiment Results and Discussion

4.1 Displacement Sensing of the CPC inductors

The coils in the CPC inductors are embroidered on two layers of fabrics and laid on top of each other. In order to measure the displacement precisely, the bottom layer of fabrics is fixed while the upper layer is moved at a 5mm spacing of each displacement step. The upper layer coil and

lower layer coil in the CPC structure are separated by a non-conductive fabric layer as an insulator.

The two terminals of the CPC inductor are connected through an adaptor to a high precision Keysight vector network analyzer E5071. The network analyzer is calibrated to the terminals of the adaptor, to eliminate the parasitic effects of the fixture. The measurement frequency is set from 1 MHz to 50 MHz with 201 points.

The setup of the displacement sensing test of the CPC inductor is illustrated in Figure 9. The bottom layer is fixed and the center of the bottom coil is assumed to be the origin, while the top coil layer is moving laterally in the y direction.

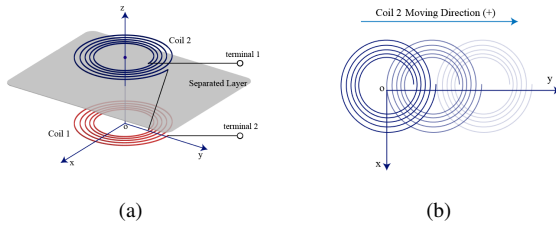


Figure 9. (a) Set up of the displacement test of the CPC coils. (b) Top coil of the CPC inductor is moving laterally in the y direction.

For the circular CPC inductor, the displacement is performed from -50 mm to 50 mm laterally with an interval of 5 mm along y axis. The total equivalent inductance at the frequency point of 13.56 MHz is measured at every displacement step and illustrated in Figure 10(a.left).

Similarly, the results from the square coil CPC inductor are shown Figure 10(b.left).

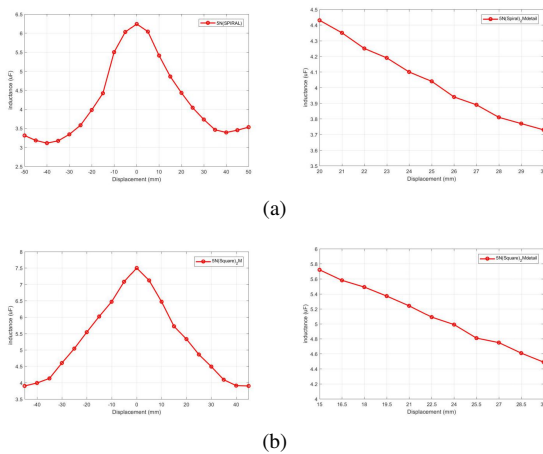


Figure 10. Inductance measurements of CPC inductor under different displacements, (a)Circular coils, (b)Square coils.

The results demonstrate that the CPC structure is an ideal sensor for the displacement between the upper layer and bottom layers. In fact, the relationship between inductance variation and displacement is quite significant. As the displacement moves from total overlap to total detachment between

the two coils, the equivalent inductance of the CPC structure varies from 6.25 uH to 3.0 uH for the circular coils, and from 7.5 uH to 4.0 uH for the squared coils.

With further comparison of the results, we find that the square-coiled CPC inductor exhibits more linearity than the circular-coiled CPC. This can be explained that the overlapping region between the squared coil changes almost linearly as the displacement moves around.

Furthermore, from Figure 10, it can be observed that different regions of the curve have quite different slopes. In fact, the sensitivity of the CPC displacement sensor can be further improved by choosing different relative locations between the coupling coils of the CPC structure.

We further test the inductance variations with the displacement ranging from 20 mm to 30 mm between the top and bottom coils of the circular CPC inductor. Within this range, the displacement is moved with an interval of 1 mm. The results are illustrated in Figure 10(a.right). It is obvious that with properly configured relative positions between the top and bottom coils, the CPC inductance exhibits a good linear relationship with the displacement. Even 1 mm of displacement shows significant variations in the inductance.

Similar results can be obtained for the squared CPC inductors. When choosing the displacement region from 15 mm to 30 mm, with an interval of 1.5 mm, the square coiled CPC also demonstrates a very sensitive relationship between the inductance variation and the small displacement steps, as shown in Figure 10(b.right).

4.2 Restorable and Directional Sensing

The top layer coil and bottom layer coil of the CPC structure can be embroidered on normal fabrics, and separated by a layer of non-conductive stretchable fabric, the displacement of the two coil layers is restorable once the external force is released. In our test, stretchable fabrics can have as much as 30% of elongations and still restore back to the original dimension. Embroidering CPC structures on stretchable fabrics will have good repeatability in the displacement sensing tests.

In addition, if the two coils of CPC are overlapping partially, the displacement sensing can be directional, i.e., as the displacement moves to different directions laterally, the inductance will be increased or decreased, indicating the direction of the movement. For example, we set the initial reference position of the circular CPC sensor at displacement $y = 25mm$, which is the location that the upper coil is half-way overlapping the bottom coil. Reducing the displacement will cause the inductance to increase, while increasing the displacement will cause the inductance to decrease. Within ± 5 mm from the reference position, the change of inductance is linear with the displacement.

4.3 Robustness

4.3.1 Resiliency to Deformation

Deformation should be taken into consideration when the CPC sensor is applied on human body, A circular CPC inductor is used to measure the inductance variations under different bending/curving conditions. The radius of the curvature is set to be 41 mm and 63 mm respectively in the

experiments. The curvature is chosen to imitate the fabric bending on arms and legs.

Results are shown in Figure 11. The displacement sensitivity is very similar between the curved (bending) conditions and normal (reference) conditions.

4.3.2 Resiliency to Human Body

To be used as on-body sensors, the human body impacts on the CPC's sensibility is also taken into account and tested. We have performed the experiments of the embroidered CPC sensors on human skins, as well as being immersed with human sweat. The results are also illustrated in Figure 11, along with the results from dry-flat CPC sensors as reference. From the figure, we can see that there is little difference in sensitivity when the CPC structure is used on human body, or in wet condition with human sweats. The results are not surprising because inductance coupling can penetrate wet substrates, therefore, inductance-based sensors should still maintain a stable performance on human bodies.

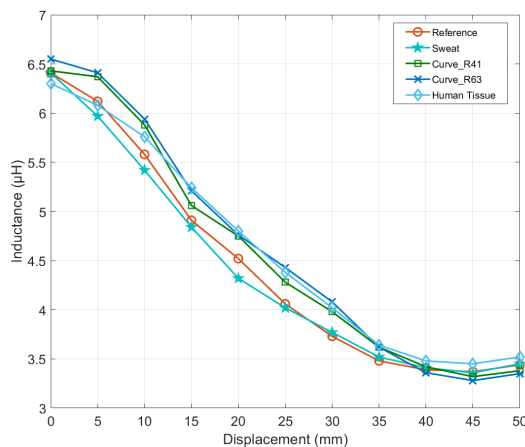


Figure 11. Human body impacts on CPC sensors.

In general, these results demonstrate that our proposed CPC structure can be used as a reliable on-body displacement sensor.

5 Future Works

The proposed embroidered displacement sensors have demonstrated great potentials for future wearable applications with the passive battery-less sensing capabilities. The scope of this paper is an early stage work exploring the characteristics of the CPC-based inductive sensor.

- The EM/mechanical properties of conductive yarns, such as resistivity, elasticity etc., as well as the parasitic elements (mostly capacitive, we believe) should be further investigated.
- The CPC structure can be used as the antenna for NFC chips. When displacement occurs, the antenna's equivalent inductance will change, and consequently modulate the coupled EM wave between the NFC tag and reader. The reader, upon demodulating the EM wave, can extract the sensing information. The complete NFC based passive sensing system is discussed in another work by the same team.

6 Conclusions

In this paper, we proposed an embroidered passive coupling planar coil (CPC) structure design that can be used as a displacement sensor. The CPC structure has two coupling coils embroidered on two separated fabrics layers. The coils are connected in series with mutual inductance formed in between. When displacement occurs between the two coils, their mutual inductance will vary, and the total equivalent inductance of the CPC structure will change accordingly. The CPC structure can be embroidered using traditional embroidery process with low-cost commercial conductive yarns. Simulation and experiments demonstrate the embroidered CPC structure can be used as a sensitive and reliable displacement sensor for many wearable applications.

7 References

- [1] S. Amendola, R. Lodato, S. Manzari, C. Occhiuzzi, and G. Marrocco. Rfid technology for iot-based personal healthcare in smart spaces. *IEEE Internet of Things Journal*, 1(2):144–152, April 2014.
- [2] N. Anandan and B. George. Design and development of a planar linear variable differential transformer for displacement sensing. *IEEE Sensors Journal*, 17(16):5298–5305, Aug 2017.
- [3] R. Del-Rio-Ruiz, J. Lopez-Garde, J. L. Macon, and H. Rogier. Design and performance analysis of a purely textile spiral antenna for on-body nfc applications. In *2017 IEEE MTT-S International Microwave Workshop Series on Advanced Materials and Processes for RF and THz Applications (IMWS-AMP)*, pages 1–3, Sep. 2017.
- [4] S. M. Djuric. Performance analysis of a planar displacement sensor with inductive spiral coils. *IEEE Transactions on Magnetics*, 50(4):1–4, April 2014.
- [5] N. J. Grabham, Y. Li, L. R. Clare, B. H. Stark, and S. P. Beeby. Fabrication techniques for manufacturing flexible coils on textiles for inductive power transfer. *IEEE Sensors Journal*, 18(6):2599–2606, March 2018.
- [6] Y. R. Jeong, J. Kim, Z. Xie, Y. Xue, S. M. Won, G. Lee, S. W. Jin, S. Y. Hong, X. Feng, Y. Huang, J. A. Rogers, and J. S. Ha. A skin-attachable, stretchable integrated system based on liquid gains for wireless human motion monitoring with multi-site sensing capabilities. *NPG Asia Materials*, 9(10):e443–e443, 2017.
- [7] O. Jonah, A. Merwaday, S. V. Georgakopoulos, and M. M. Tentzeris. Spiral resonators for optimally efficient strongly coupled magnetic resonant systems. *Wireless Power Transfer*, 1(1):21–26, 03 2014.
- [8] Y. Liu, L. Xu, Y. Li, and T. T. Ye. Textile based embroidery-friendly rfid antenna design techniques. In *2019 IEEE International Conference on RFID (RFID)*, pages 1–6.
- [9] N. Misron, L. Q. Ying, R. N. Firdaus, N. Abdullah, N. F. Mailah, and H. Wakiwaka. Effect of inductive coil shape on sensing performance of linear displacement sensor using thin inductive coil and pattern guide. *Sensors*, 11(11):10522–10533, 2011.
- [10] E. Moradi, T. Bjorninen, L. Ukkonen, and Y. Rahmat-Samii. Effects of sewing pattern on the performance of embroidered dipole-type rfid tag antennas. *IEEE Antennas and Wireless Propagation Letters*, 11:1482–1485, 2012.
- [11] Y. Ouyang and W. J. Chappell. High frequency properties of electro-textiles for wearable antenna applications. *IEEE Transactions on Antennas and Propagation*, 56(2):381–389, Feb 2008.
- [12] J. S. Roh, Y. S. Chi, J. H. Lee, S. Nam, and T. J. Kang. Characterization of embroidered inductors. *Smart Materials and Structures*, 19(11):115020, 2010.
- [13] A. Tsolis, W. G. Whittow, A. A. Alexandridis, and J. C. Vardaxoglou. Embroidery and related manufacturing techniques for wearable antennas: Challenges and opportunities. *Electronics*, 3(2):314–338, 2014.
- [14] Z. Wang, L. Zhang, Y. Bayram, and J. L. Volakis. Embroidered conductive fibers on polymer composite for conformal antennas. *IEEE Transactions on Antennas and Propagation*, 60(9):4141–4147, Sep. 2012.